Mesophases of (Bio)Polymer–Silica Particles Inspire a Model for Silica Biomineralization in Diatoms**

Engel G. Vrieling,* Theo P. M. Beelen,
Rutger A. van Santen, and Winfried W. C. Gieskes*

Diatoms, the dominant component of the plant biomass in marine and freshwater environments, are best known for their species-specific cell-wall architecture of amorphous silica.[1, 2] Synthetic silica-based materials are widely used for industrial purposes, but if nature could be mimicked innovative tailor-made silicas could be produced that approach the architectures of diatom exoskeletons.[3–5] Silica formation in diatoms seems to be mediated by peptides and polyamines,[6–8] but how short-term processes control structure-directed silica deposition remains unknown. The size range of the siliceous units and the intracellular location of silica deposition prohibit in situ analysis, while delicate silica intermediates are altered or damaged during isolation and sample preparation prior to structural or biophysical analysis.

Noninvasive X-ray scattering approaches are promising for the study of silica transformation in situ.[9, 10] To gain insight into silica aggregation and transformation on much larger length scales (up to 6500 nm) in comparison to the well-known silica chemistry on smaller length scales (< 10 nm),[11] we examined X-ray scattering of silica structures at ultrasmall angles (USAXS), which allows reliable statements regarding the geometry and interaction of scattering sources.

Silica formation in diatoms was approximated by synthesizing silica from acidified water glass (tetraethyl orthosilicate is not a natural silica source) in the presence of structure-directing agents; the concentration of dissolved silica and the pH of the solvent were comparable to conditions during silica deposition inside diatoms.[12] All syntheses were monitored in situ at room temperature and at 90 °C to accelerate the aging of silica; all end-points were compared with that of a template-free control. In the control (Figure 1a), silica aggregates formed the expected xerogel by reaction-limited cluster–cluster aggregation (RCCA).[13] The observed slope in the $\lg I - \lg q$ plot of the aged xerogel is -2.58 (Figure 1a), which corresponds to a mass-fractal dimension D_m of 2.58. Surface fractals [D_s, where $D_s = 6 - (-\text{slope})$] are excluded, since they are only physically significant if $2 < D_s < 3$.[13] The USAXS spectrum of the xerogel revealed no transition points for defining the radius of gyration R_g or primary particle size r_p. Therefore, it can be concluded[9, 14] that the aggregates were large ($R_g > 6000$ nm with $d = 2\pi q^{-1}$) and composed of primary particles with $r_p \ll 30$ nm.[9, 10]

Porous silicas can be prepared when polymers are used as structure-directing agents.[15, 16] In silica directed by poly(ethylene imine) (PEI) distinct straight $\lg I - \lg q$ lines were present (bottom line Figure 1b), with a transition point at $q \approx 0.05$ nm^{-1}. The slope at $q > 0.05$ nm^{-1} was -2.63, which almost equals that of the above-mentioned xerogel. However, rather large fractal particles may have formed by interaction of silica with C–C–NH_2 branches of PEI. The size (R_g) of these fractal particles at $q = 0.05$ is approximately 125 nm, roughly that expected with PEI ($M_w = 200\,000$). At $q < 0.05$ nm^{-1} a less steep slope (-2.03) indicates formation of much larger aggregates ($R_g > 6000$ nm), similar to those in the xerogel. However, when the 125-nm-sized PEI–silica particles are used for the formation of these large aggregates, a strong influence of diffusion limitation results in a much less dense network and a lower D_m (2.03). In silica directed by poly(ethylene glycol) (PEG) a totally different scattering pattern was observed (upper line in Figure 1b), that is, one straight line with slope of -4.0. This implies the presence of only large ($R_g > 6000$ nm), smooth, nonfractal spherical or vesicle-shaped particles.

Proteinaceous compounds have also been reported to serve as templates.[17] We used horseradish peroxidase (HRP) and myoglobin (MG) as models, because functional diatomaceous peptides (e.g., silaffins bearing essential polyamine-modified lysine residues[6–8]) cannot be obtained readily. Because of their size, polyamines and silaffins become completely encapsulated and can no longer direct silica transformations,[18] although they efficiently induce silica precipitation.[6, 7] With HRP a straight line covering a wide q range ($0.001 < q < 0.2$ nm^{-1}) was obtained (bottom line in Figure 1c). Similar to the xerogel and PEI-directed silica, this indicates the formation of large fractal aggregates ($R_g >$ 6000 nm). However, with HRP the aggregation process resulted in a fractal dimension ($D_m = 2.20$) between the values found for the xerogel and PEI-directed silica, but corresponding to the intermediate size of HRP molecules between those of PEI and primary silica particles. In contrast, the MG-directed silica showed multiple straight-line regions (upper line Figure 1c). At $q > 0.024$ nm^{-1} the slope of -2.72 corresponds to fractal MG–silica aggregates of about 260 nm in size (R_g at $q = 0.024$). At $q < 0.003$ nm^{-1} the slope of -2.00 corresponds to much larger diffusion-limited (fractal) aggregates of MG–silica particles ($R_g > 6000$ nm). The short intermediate section ($0.003 < q < 0.024$ nm) with a slope of -3.40 represents a transition region.

[*] Dr. E. G. Vrieling,[+] Dr. W. W. C. Gieskes
Department of Marine Biology
Center for Ecological and Evolutionary Studies
University of Groningen, Biological Center
P.O. Box 14, 9750 AA Haren (The Netherlands)
Fax: (+31) 50-363-2261
E-mail: e.g.vrieling@chem.rug.nl
w.w.c.gieskes@biol.rug.nl
Dr. ir. T. P. M. Beelen, Prof. Dr. ir. R. A. van Santen
Laboratory of Inorganic Chemistry and Catalysis
Schuit Institute of Catalysis, Eindhoven University of Technology
P.O. Box 513, 5600 MB, Eindhoven (The Netherlands)
Fax: (+31) 40-245-5054

[+] New address:
Groningen Biomolecular Sciences and Biotechnology Institute
University of Groningen, Nijenborgh 4
9747 AG Groningen (The Netherlands)
Fax: (+31) 50-363-4165

[**] We thank Dr. T. Narayanan, European Synchrotron Radiation Facility (ESRF, Grenoble, France), and C. Houssin for assistance during measurements. The European Committee granted beamtime (proposal no: SC 595). A. J. van Bennekom of the Netherlands Institute for Sea Research (NIOZ) provided the biogenic silica. E.G.V. was supported by the Netherlands Technology Foundation (STW; grant GFc4983), which is subsidized by the Netherlands Organization for the Advancement of Pure Research (NWO).

  1433-7851/02/4109-1543 $ 20.00+.50/0

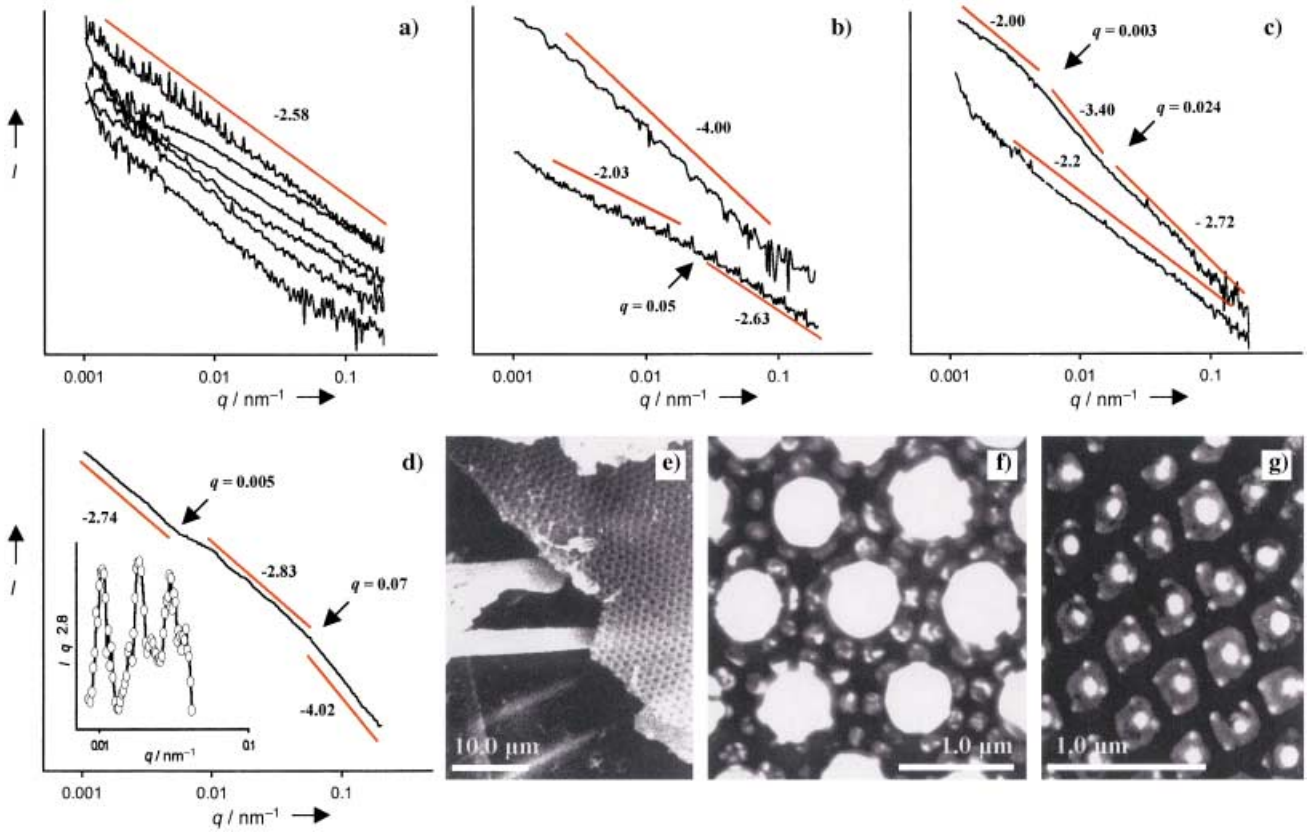

Figure 1. USAXS spectra of time-dependent silica transformations presented as plots of $\lg I$ (scattering intensity) vs $\lg q$ (scattering vector). a) The template-free control experiment resulted in a xerogel; aging at 90 °C (upper 3 lines) followed growth at RT (bottom lines). b, c) Final spectra of template-directed silica syntheses: b) PEI- (bottom line) and PEG-directed silica (upper line), and c) HRP- (bottom line) and MG- directed silica (upper line). d) USAXS spectrum of dried silica from the diatom *Odontella sinensis*, showing distinct regions with slopes of -2.7, -2.8, -4.0. To indicate the position of the small oscillations clearly (inset), the disturbing influence of the slope is cancelled by plotting $Iq^{2.8}$ vs $\lg q$. For clarity, transition points are indicated with arrows, and red lines show the determined slopes. e – g) Electron micrographs at various magnifications of *O. sinensis* silica showing the pore dimensions observed by USAXS in valves (e, f) and girdle bands (g).

The physical principles of USAXS, informative for dimensions and fractal behavior of silica particles in solution, are also applicable to silica powders, where scattering is caused by pores in the solid.[1, 13] Analysis of silica of the diatom *Odontella sinensis* (Figure 1 d) revealed a pattern as expected for porous diatomaceous silica, which typically has more than one pore dimension and shape.[1, 2] Electron microscopy (EM) confirmed a distribution of a similar range of pores in the same material (Figure 1 e – g). As expected, the Porod region at $q > 0.08\ \mathrm{nm}^{-1}$ shows a slope of -4.0 in the $\lg I - \lg q$ plot due to scattering of smaller spherical pores. The two other regions in the spectrum, with slopes of -2.8 ($0.01 < q < 0.06\ \mathrm{nm}^{-1}$) and -2.7 ($q < 0.005\ \mathrm{nm}^{-1}$), are here ascribed to combined contributions of several types of pores that are different in size and shape. As observed earlier,[1] oscillations (inset of Figure 1 d) are also present, although at much larger length scales, between $15 < d < 600$ nm ($0.01 < q < 0.4\ \mathrm{nm}^{-1}$). These oscillations are interpreted as structure factors resulting from well-organized distributions of pores, as could be observed by EM (Figure 1 e – g).

Previous investigations only demonstrated that organic templates build different microporous silicas.[9, 10, 15–17] Here each polymer or peptide induces formation of distinct silica structures over length scales spanning five decades in size. This may be the key to an explanation of how diatoms achieve their intricate silica cell-wall architectures, in which the hierarchy of the very different pores of each species covers a similar size range. If diatoms resemble the above-mentioned systems in that they must create silica aggregates whose pores are much larger than a single template molecule, it may be that clustered template molecules come into effect for the larger dimensions, especially since small organic molecules (potentially silaffins, polyamines, and block polypeptides[6–8, 17]) become completely and irreversibly encapsulated inside silica sol – gels.[18] In experiments with PEG the formation of silica is influenced by hydrophobic interactions between PEG and the growing silica, which induce transfer of PEG and silicyl monomers and oligomers from the solvent into a silica-rich phase, a process called phase separation.[15] The same was observed during the formation of MCM materials[16] and can be predicted for polymer – nanoparticle composites.[19]

In our syntheses, growing silica triggers phase separation by addition of silicyl monomers and template molecules to growing silica – template intermediates, while mesophases can direct formation of larger silica structures. This mechanism is the basis of our hypothesis (Figure 2) of how development of the silica architecture proceeds inside the silica-deposition

  1433-7851/02/4109-1544 $ 20.00+.50/0

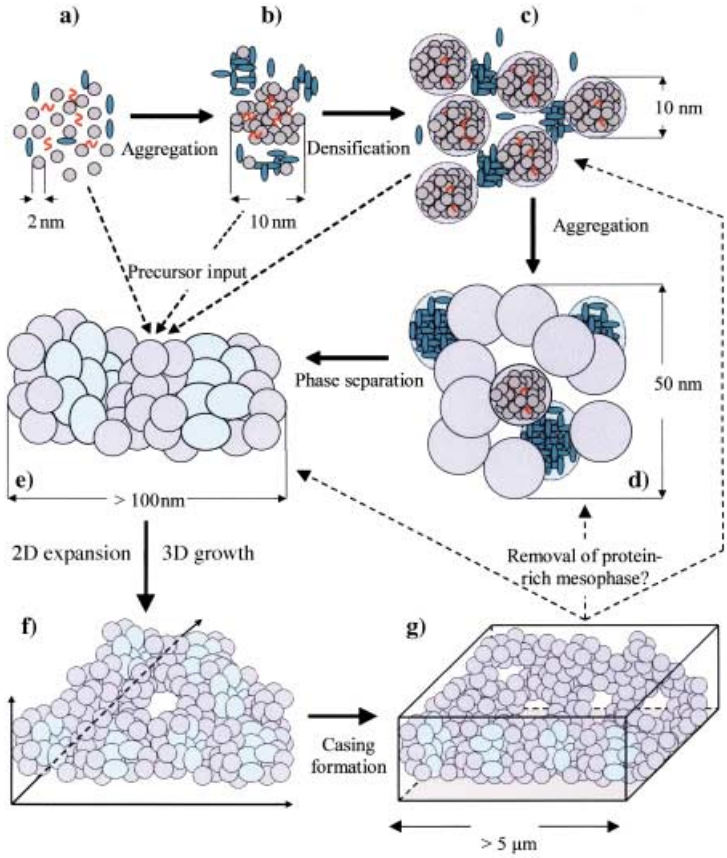

Figure 2. The proposed model of mesophase silica polymerization in diatoms, based on the polymer- and peptide-directed silica syntheses. a) In the immature silica deposition vesicle (SDV) small peptides and/or polyamines (red curved structures), larger organic molecules (green ellipsoids), and silica precursors are present. The latter form small silica sols (gray spheres). b) Silaffins[6, 8] and polyamines,[7] as well as the environmental pH and continuous import of silica precursors in the SDV,[12] induce fast aggregation of silica. In this process the small organic molecules become completely encapsulated,[18] while larger peptides interact with the silica and each other. c) Aggregates of silica/silaffins/polyamines densify to larger silica structures (blue circles), which interact with growing aggregates of the larger peptides (the mesophase precursors). d) Continuing aggregation forms larger silica/silica and silica/peptide aggregates (greenish ovals) with structures of about 50 nm in size. e) Densified mesophase particles grow to sizes larger than 100 nm. f) Following continuous input of peptides and silica precursors to the SDV, two-dimensional (2D) expansion and three-dimensional (3D) growth is realized. g) Since large peptides do not remain after the wall has been completed and covered by the casing, we assume that they are somehow removed.

vesicle (SDV) of diatoms. At the onset of valve formation (Figure 2a) silica precursors are transported to the SDV, where the small silaffins and polyamines[6–8] in an acidic SDV[12] induce rapid precipitation of silica. Larger peptides interact with the formed silica sols and each other (Figure 2b). Beyond this stage silica densifies, and the larger peptides form large templates as a mesophase (Figure 2c). The larger particles continue to aggregate (Figure 2d) and to densify further (Figure 2e). The dimension of the mesophases depends on the species-specific type or set of peptides that mediate silica polymerization. Continuous delivery of precursors to the SDV allows it to expand two-dimensionally and grow in the third dimension (Figure 2f). When silica parts are completed, we assume that the proteinaceous mesophase somehow is removed in the course of covering the silica with a protective organic casing (Figure 2g). The assumption of template removal originates from the fact that the few peptides found to be associated with, but not encapsulated in, mature silica cell walls do not play a role in silica polymerization.[20, 21]

Our model suggests that proteinaceous mesophases behave like the wax used in the "cire perdue" (lost wax) method of producing bronze castings. Once silica has been constructed, the proteinaceous phase is removed, leaving a cavity (pore) that is much larger than a single peptide molecule would ever leave. Genetically determined combinations of peptides would generate the differences in pore patterns that are so typically species-specific in diatom cell walls. The next step now is to collect supporting evidence for our hypothesis by following silica syntheses in vitro by using diatomaceous peptides or closely related synthetic compounds.

Experimental Section

Wet silica gels, both with and without templates, were prepared by dropwise addition of 10 mL of water glass solution (6.75% (w/v) SiO_2) to a stirred mixture of HCl (15 mL, 1.0 M), water (10 mL), and template (0.43 g). The templates were poly(ethylene glycol) (PEG; $M_W = 2000$), poly(ethylene imine) (PEI; $M_W = 200000$), myoglobin (MG; $M_W = 17$ kDa), and horseradish peroxidase (HRP; $M_W =$ 40 kDa). Immediately after preparation the mixture was transferred to a rotating cell with mica windows (Ø10 mm) and a Teflon spacer (thickness 1 mm) for time-resolved USAXS analysis.[10] After 10–12 h at RT the gels were aged in situ at 90 °C, and again monitored (10–12 h). Silica powder of the diatom *Odontella sinensis* was prepared by low-temperature ashing.[22] USAXS experiments were performed at the high-brilliance beamline ID02 ($\lambda = 0.099$ nm) at the ESRF (Grenoble, France) by using a Bonse-Hart camera and a configuration with two analyzer crystals to avoid desmearing.[23] The q range, calibrated with silver behenate, was $0.001 < q < 0.3$ nm^{-1} ($21 < d < 6280$ nm). Several scans (4–5) over successive 2θ ranges with a sufficient overlap were recorded with different degrees of attenuation of the incident X-ray beam, so that the intensities on the detector were in the linear range. A complete spectrum could be recorded within 15 min. Data sets were corrected for the influence of the rocking curve produced by the setup, background scattering, the small intensity fluctuations of the beam, and the absorption by the reaction mixture. Due to the strong scattering of silica in aggregates and gels, the contribution of water scattering was negligible.[10] The final scattering intensities were plotted as $\lg I$ vs $\lg q$, with I in arbitrary units and q in nm^{-1}; the latter corresponds to $d = 2\pi q^{-1}$ (in nm).

Received: June 13, 2001
Revised: January 9, 2002 [Z17287]

[1] E. G. Vrieling, T. P. M. Beelen, R. A. van Santen, W. W. C. Gieskes, *J. Phycol.* **2000**, *35*, 1044–1053.
[2] F. E. Round, R. M. Crawford, D. G. Mann, *Diatoms, The Biology and Morphology of the Genera*, Cambridge University Press, Cambridge, UK, **1990**.
[3] C. M. Zaremba, G. D. Stucky, *Curr. Opin. Solid State Mater. Sci.* **1996**, *1*, 425–429.
[4] D. E. Morse, *TIBTECH* **1999**,*7*, 230–232.
[5] E. G. Vrieling, T. P. M. Beelen, R. A. van Santen, W. W. C. Gieskes, *J. Biotechnol.* **1999**,*70*, 39–51.
[6] N. Kröger, R. Deutzmann, M. Sumper, *Science* **1999**, *286*, 1129–1132.
[7] N. Kröger, R. Deutzmann, C. Bergsdorf, M. Sumper, *Proc. Natl. Acad. Sci. USA* **2000**, *97*, 14133–14138.
[8] N. Kröger, R. Deutzmann, M. Sumper, *J. Biol. Chem.* **2001**, *276*, 26066–26070.

  1433-7851/02/4109-1545 $ 20.00+.50/0

[9] P. W. J. G. Wijnen, T. P. M. Beelen, K. P. J. Rummens, H. C. P. L. Saeijs, J. W. de Haan, L. J. M. van de Ven, R. A. van Santen, *J. Col. Interf. Sci.* **1991**, *145*, 17–32.
[10] P.-P. E. A. de Moor, T. P. M. Beelen, R. A. van Santen, *J. Phys. Chem. B* **1999**, *103*, 1639–1650.
[11] R. K. Iler, *The Chemistry of Silica: Solubility, Polymerization, Colloid and Surface Properties, and Biochemistry*, Wiley, New York, **1979**.
[12] E. G. Vrieling, T. P. M. Beelen, W. W. C. Gieskes, *J. Phycol.* **1999**, *35*, 548–559.
[13] C. J. Brinker, G. Scherer, *Sol-Gel Science*, Academic Press, New York, **1990**.
[14] T. P. M. Beelen, W. Shi, G. R. Morrison, H. F. van Garderen, M. T. Browne, R. A. van Santen, E. Pantos, *J. Coll. Interf. Sci.* **1997**, *185*, 217–227.
[15] R. Takahashi, K. Nakanishi, N. Soga, *J. Sol-Gel Sci. Technol.* **2000**, *17*, 7–18.
[16] S. Biz, M. Ocelli, *Catal. Rev. Sci. Eng.* **1998**, *40*, 329–407.
[17] J. N. Cha, G. D. Stucky, D. E. Morse, T. J. Deming, *Nature* **2000**, *403*, 289–292.
[18] G. Iqbal, A. Ballesteros, *TIBTECH* **2000**, *18*, 282–296.
[19] R. B. Thompson, V. V. Ginzburg, M. W. Matsen, A. C. Balazs, *Science* **2001**, *292*, 2469–2472.
[20] W. H. van de Poll, E. G. Vrieling, W. W. C. Gieskes, *J. Phycol.* **1999**, *35*, 1044–1053.
[21] N. Kröger, R. Wetherbee, *Protist* **2000**, *151*, 263–273.
[22] A. J. van Bennekom, J. H. F. Jansen, S. J. van der Gaast, J. M. van Iperen, J. Pieters, *Deep Sea Res.* **1989**, *36*, 173–190.
[23] O. Diat, P. Bösecke, J. Lambard, P.-P. E. A. de Moor, *J. Appl. Crystallogr.* **1997**, *30*, 862–886.

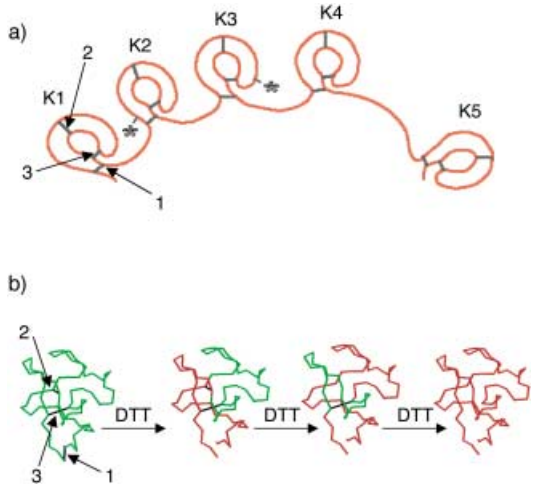

Figure 1. a) Schematic representation of the Ang(1–5) structure with the triple-loop topology of its five Kringle domains (K1–K5), determined in each case by a sequence of three disulfide bonds: cys1–cys80 (1), cys22–cys63 (2), and cys51–cys75 (3). The two asterisks (*) indicate the position of an additional, inter-Kringle disulfide bond. b) Pathway of the sequential reduction of the most exposed (1) and then of the more interior (2) and (3) bonds. This reduction pathway leads to gradually lengthening topological loops (red) that are exposed to the force exerted by the SFM tip at the two ends of the Kringle domain.

The Mechanical Properties of Human Angiostatin Can Be Modulated by Means of Its Disulfide Bonds: A Single-Molecule Force-Spectroscopy Study**

Yasser Bustanji and Bruno Samorì*

Human angiostatin 1–5 [Ang(1–5)], a 57 kDa proteolitic fragment of human plasminogen, consists of five compact globular modules called Kringle domains with very similar gross architecture and remarkable sequence homology. They are built around a hydrophobic core and exhibit a triple-loop topology defined by three internal disulfide bonds: cys1–cys80 (1), cys22–cys63 (2), and cys51–cys75 (3) (Figure 1a).[1] Here we report on a single-molecule force-spectroscopy study that shows how the redox environment can control the topology and mechanical properties of angiostatin by modifying the extent of pairing of the internal disulfide bonds.

Ang(1–5) molecules were deposited on a polystyrene surface; the tip of a scanning force microscope (SFM) was brought into contact with this surface and retracted after reaching a force of 1 nN. This cycle was repeated many hundreds of times, first under phosphate buffer saline (PBS), and then under different reducing conditions by using dithiothreitol (DTT) in concentrations ranging from 5 to 100 mM. Whenever the tip physically adsorbed and picked up a chain segment of an Ang(1–5) molecule, a molecular bridge was established between the two moving surfaces, and the force acting on this bridge was plotted versus the tip displacement in force curves such as those in Figure 2.

Two representative curves, recorded under PBS buffer prior to any addition of reducing agent, are shown in Figure 2a. Their profiles are very irregular and typical of deadsorption processes of globular or short inextensible proteins.[2] These curves do not exhibit the characteristic sawtooth pattern that was previously recognized to be typical of multimodular proteins, and first demonstrated by Gaub and co-workers to result from the sequential stepwise unfolding of their individual domains.[3] This was due to the fact that Ang(1–5) disulfide bonds acted as mechanical barriers to mechanical unfolding. In fact, being covalent bonds, they can withstand forces up to a few nanonewtons,[4] that is, much higher than those involved in the experiments reported here, which were in the range of 30–150 pN. Therefore, the mechanical stress exerted on the disulfide bonds, both under nonreducing and reducing conditions (see below), could never succeed in breaking any of them.

The PBS buffer in the fluid cell was then replaced with a 5 mM DTT solution, and force curves were recorded 30 min after DTT injection. This experiment was also performed with 50 and 100 mM DTT, and in the latter case the incubation time was doubled. The force curves recorded under these three sets of reducing conditions exhibited the characteristic sequences of sawtooth peaks (Figure 2b–d). Each peak resulted from the unfolding of a single module. Each Ang(1–5) module could unfold until an internal unreduced disulfide bond was met along its unfolding pathway. In fact only the disulfide

[*] Prof. B. Samorì, Dr. Y. Bustanji
Dipartimento di Biochimica, Università di Bologna
Via Irnerio 48, 40126 Bologna (Italy)
Fax: (+39) 051-2094387
E-mail: samori@alma.unibo.it

[**] This work was supported by Programmi Biotecnologie legge 95/95 (MURST 5%), and MURST PRIN Progetti Biologia Strutturale 1997–1999 and 1999–2001.

  1433-7851/02/4109-1546 $ 20.00+.50/0